

Cite this: *Chem. Commun.*, 2012, **48**, 1854–1856

www.rsc.org/chemcomm

Surfactant-free preparation of supported cubic platinum nanoparticles†

Zhenmeng Peng,^a Christian Kisielowski^b and Alexis T. Bell^{*ab}

Received 9th November 2011, Accepted 13th December 2011

DOI: 10.1039/c2cc16962b

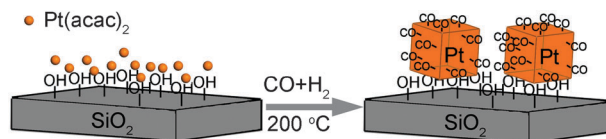
A novel method has been developed for preparing supported cubic platinum nanoparticles. Carbon monoxide and hydrogen are used to reduce platinum precursors present at a solid–gas interface and to control the shape of the growing Pt nanoparticles. By avoiding the use of any organic agents in the synthesis, cubic Pt particles free of hydrocarbons are formed, thereby avoiding possible contamination of the catalyst surface. The approach used is simple and readily scalable.

Supported platinum catalysts are used extensively, particularly for the reforming of hydrocarbon and the reduction of oxygen in fuel cells.^{1–4} Recent work has shown that the catalytic activity and selectivity of such catalysts can be altered significantly by the nature of the Pt facets exposed.^{5–7} For example, Pt nanocubes have been found to be highly active for ring-opening hydrogenation of pyrroles resulting in the highly selective formation of n-butylamine.⁸ Cubic Pt particles also exhibit high activity and selectivity for the hydrogenation of benzene to cyclohexane, without the formation of cyclohexene observed when Pt has other shapes.⁹ The electro-oxidation of methanol has also been found to be more active on Pt (100) than on Pt (111).¹⁰ These findings have stimulated the exploration of new methods for preparing Pt nanoparticles with well-defined shape.^{11,12} Various wet chemical approaches have been reported recently for making shaped Pt nanoparticles.^{13–17} Capping agents, such as sodium polyacrylate,¹⁸ polyvinylpyrrolidone,^{19,20} and metal carbonyls,^{21,22} have been found to be effective for controlling the particle shape. More recently, carbon monoxide gas has been observed to help generate Pt facets in non-hydrolytic solutions containing oleylamine/oleic acid.^{23–25} Excessive amounts of organic agents are employed in these synthetic methods, often leading to severe contamination problems and requiring complete removal of hydrocarbons from the Pt surface before it becomes catalytically active. Moreover, the complexity of such preparative procedures and the difficulties in scaling them up have limited the use of colloidal methods to fundamental studies and made them less useful for real applications.

^a Department of Chemical and Biomolecular Engineering, University of California, Berkeley, CA 94720, USA

^b Joint Center for Artificial Photosynthesis, Lawrence Berkeley National Laboratory, 1 Cyclotron Road, Berkeley, CA 94708, USA. E-mail: bell@cchem.berkeley.edu; Fax: +1 510 642 4778

† Electronic supplementary information (ESI) available: SEM and EDX of Pt(acac)₂/SiO₂, TEM, HRTEM, HAADF-STEM, PXRD, and FTIR of as-prepared Pt/SiO₂, *in situ* FTIR of reducing Pt(acac)₂/SiO₂, and experimental details. See DOI: 10.1039/c2cc16962b



Scheme 1 A schematic illustration of the formation of cubic Pt nanoparticles on a SiO₂ support in the presence of CO and H₂ gases.

Here we report a facile, one-step approach for making supported cubic Pt nanoparticles without the need for organic reducing/capping agents (see ESI† for details). The whole preparation process is carried out using only gas-phase reducing agents. Briefly, platinum acetylacetonate is first dissolved in acetone, impregnated onto a pretreated silica support, and then dried under vacuum. Energy dispersive X-ray (EDX) analyses suggest that the Pt precursor is distributed uniformly on the surface of SiO₂ (Fig. S1, ESI†). The solid is subsequently heated to 200 °C for 1 h in a gas mixture of CO and H₂ (Scheme 1). A uniform dispersion of Pt nanocubes on the SiO₂ is obtained by this means (Fig. S2, ESI†).

Fig. 1a and b show transmission electron microscopy (TEM) and high-angle annular dark field scanning TEM

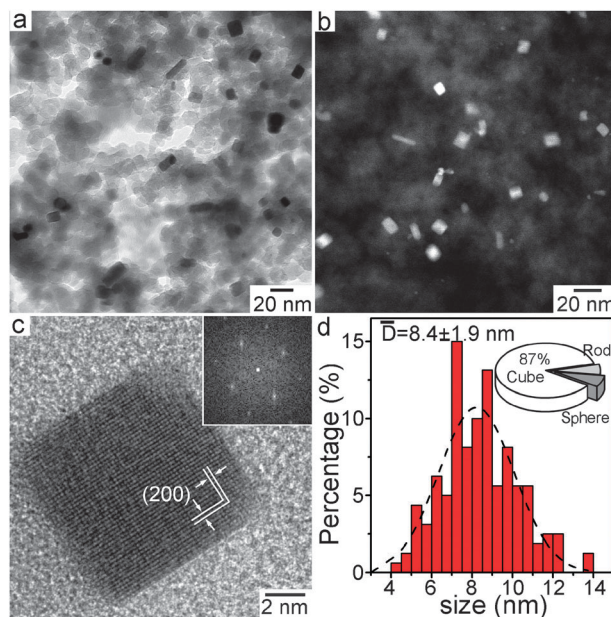


Fig. 1 (a) TEM, (b) STEM, (c) HRTEM and FFT pattern, and (d) size distribution of as-prepared cubic Pt/SiO₂ following reduction for 1 h at 200 °C in a CO/H₂ (25/5 cm³ min⁻¹) mixture.

(HAADF-STEM) images of the as-made Pt nanocubes supported on SiO₂. Most of the particles are seen to have straight edges with sharp corners. The high-resolution TEM (HRTEM) image of a single Pt nanocube shows lattice fringes parallel to its straight edges (Fig. 1c). The measured interplanar spacing of 1.96 Å matches that of Pt (200) planes for the face-centered cubic (fcc) structure and demonstrates that the cubic Pt nanoparticles are primarily enclosed by (200) surfaces. The fast Fourier transform (FFT) pattern of the lattice image exhibits a four-fold symmetry, consistent with the projection of the fcc structure from its [001] direction (see inset of Fig. 1c). Statistical analysis of the sample shows that 87% of the Pt particles are cubic in shape under the specified reaction conditions (Fig. 1d). The byproducts consist of some spheres, rectangular structures and twin-planed rods (Fig. S3, ESI†). We believe that the growth of rectangular shaped particles is attributable to the presence of rough end surfaces that contain steps which facilitate faster crystal growth than would be expected for perfect (200) planes (Fig. S3a, ESI†). The appearance of Pt rods and spheres is possibly due to formation of twin planes in the early stages of crystal growth, which result in the exposure of (111) planes and thus a change in the pattern of crystal growth (Fig. S3b, ESI†). The distribution of edge sizes of the Pt particles follows a narrow Gaussian distribution with an average edge size of 8.4 ± 1.9 nm (Fig. 1d). The size is in a reasonable agreement with that estimated from the (200) X-ray diffraction peak using the Scherrer equation (Fig. S4, ESI†).

The formation of cubic Pt/SiO₂ can be achieved in the temperature range of 150 to 250 °C, but at lower temperatures Pt cannot be reduced efficiently (Fig. S5, ESI†). The Pt cubes produced at the temperature of 250 °C have round corners and less sharp edges than those produced at lower temperatures. When the reduction temperature is raised to 300 °C, the particles become spherical. These findings suggest that the cubic shaped particles are thermodynamically unstable at elevated temperatures. The concentrations of CO and H₂ were adjusted systematically to study the effects of reducing gas composition on the final product. Both gases were found to be crucial in the formation of Pt nanocubes (Fig. S6, ESI†). The CO/H₂ ratio did not have a significant effect on the final product for flows in the range of 25/5 to 10/20 cm³ min⁻¹; in each case cubic Pt particles of similar size were formed. Most of the particles obtained in the presence of pure CO, however, were dramatically different and much smaller in size (Fig. S6a, ESI†). On the other hand, large spherical particles were observed when H₂ was used alone (Fig. S6d, ESI†). These findings suggest that H₂ facilitates the transport of Pt precursors to their growth sites. The small Pt particles formed in pure CO are probably due to a restricted diffusion of the precursors on the support in the absence of H₂. The spherical shape and non-uniform size of the formed Pt in pure H₂ suggests that CO mediates the growth of the Pt and shapes them into cube. The formation of a cubic shape is very likely associated with preferential chemisorption of CO on Pt (100), thereby modifying the growth kinetics.^{23–25} Previous experimental and theoretical studies have shown a stronger binding of CO molecules to Pt (100) than to other low-indexed facets.^{24,26} The strongly adsorbed CO will inhibit the growth of (100) planes, resulting in these surfaces

becoming the bounding surfaces of the final particles.^{14,16} It was also observed that CO alone, but not H₂, could reduce Pt efficiently at 150 °C, suggesting the CO plays the primary role in the reduction process.²³

The effects of support pretreatment were examined by dehydrating SiO₂ at different temperatures. Pt cubes with a smaller size were obtained when SiO₂ was pretreated at temperatures below 300 °C. Dehydration at this temperature leaves a larger surface concentration of silanol groups than pretreatment at 700 °C (Fig. S7a, ESI†), and suggests that the silanol groups are involved in the Pt nucleation and growth. Cubic Pt can also be produced on an amorphous carbon support, which has abundant hydroxyl/carboxyl groups on its surface (Fig. S7b, ESI†). In contrast, only small particles were formed when non-protonated Al₂O₃ and TiO₂ supports were used (Fig. S7c and d, ESI†). These results indicate the importance of surface groups, which may work in concert somehow with H₂ to assure the efficient movement of Pt precursors on the support.

The reduction of Pt(acac)₂/SiO₂ to form cubic Pt/SiO₂ was studied by stopping the reaction at designated temperatures and times and then characterizing the sample by TEM. Some of the Pt had already been reduced, primarily in the form of small nanoparticles, when the temperature was raised to 180 °C (Fig. S8, ESI†). These small Pt entities appear to act as seeds and quickly grew into cubes as the temperature was further increased. Cubic Pt particles of similar size compared to the final product were obtained shortly after the temperature was raised to 200 °C, suggesting that reduction occurs very rapidly at this temperature. *In situ* Fourier transform infrared (FTIR) spectra of adsorbed CO were acquired as a function of time as reduction proceeded. Fig. S9 (ESI†) and Fig. 2a show the original FTIR spectra and those obtained after background subtraction, respectively. The band at 2093 cm⁻¹ is due to linearly chemisorbed CO on metallic Pt. This feature was not observable until the sample had been heated to ~180 °C, indicating that only a minimal amount of Pt had been reduced below this temperature. A significant growth in the intensity of the band was observed with further increase in the temperature. Concurrently, the peaks associated with acetylacetonate groups, located at 1553, 1526, and 1381 cm⁻¹, diminished in intensity as a consequence of the decomposition of the organic groups. The absence of peaks at these positions after reaction is indicative of complete removal of the acetylacetonates (Fig. S10, ESI†).

The amount of chemisorbed CO on Pt was used as a measure of the extent of Pt reduction, and was calculated by integrating the area under its peak. The normalized data reached its maximum after ~40 min of reaction at 200 °C, suggesting complete reduction of Pt at this temperature and time (Fig. 2b). The extent of Pt reduction, X_{Pt} , and the rate of reduction, dX_{Pt}/dt , over the course of reaction at 200 °C were estimated from Fig. 2b and are shown in Fig. 2c. The extent of Pt reduction was calculated based on their correlation between the amount of chemisorbed CO and the assumption that Pt nanocubes are grown from cubic seeds after a burst of nucleation (see Fig. S8 and ESI† for details). The curve for dX_{Pt}/dt can be fitted to an exponential decay characteristic of a diffusion-controlled reaction, suggesting that the diffusion of Pt precursors on the SiO₂ surface may be the rate-determining step in their transformation into Pt cubes (Fig. 2c).^{27–29}

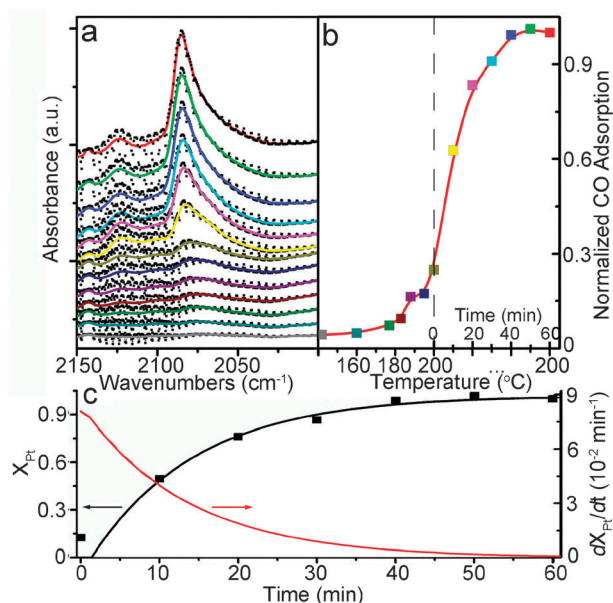


Fig. 2 (a) *In situ* FTIR spectra and (b) normalized chemisorption of CO, and (c) calculated extent of Pt(acac)₂/SiO₂ reduction (X_{Pt}) and rate of reduction (dX_{Pt}/dt) at 200 °C upon heating the sample at 3 °C min⁻¹ to 200 °C and then keeping it at this temperature for 1 h in 25/5 cm³ min⁻¹ CO/H₂.

In summary, a novel approach has been developed for the preparation of cubic Pt nanoparticles using a gas mixture of CO and H₂. Experimental studies show that the solid–gas interface reaction begins with initial formation of Pt nuclei, which grow into cubes through the surface diffusion of Pt precursors to the nuclei. Both H₂ and the support silanol groups are crucial in facilitating the movement of the Pt precursors. CO is primarily responsible for reducing Pt, mediating its growth and shaping it into cubes.

This work was supported by a grant from Chevron Energy Technology Company. The authors acknowledge support of the National Center for Electron Microscopy, Lawrence Berkeley Lab, which is supported by the U.S. Department of Energy under Contract DE-AC02-05CH11231.

Notes and references

- 1 R. Burch, J. P. Breen and F. C. Meunier, *Appl. Catal., B*, 2002, **39**, 283–303.
- 2 V. Galvita, G. Siddiqi, P. P. Sun and A. T. Bell, *J. Catal.*, 2010, **271**, 209–219.
- 3 H. A. Gasteiger, S. S. Kocha, B. Sompalli and F. T. Wagner, *Appl. Catal., B*, 2005, **56**, 9–35.
- 4 A. K. Santra and D. W. Goodman, *Electrochim. Acta*, 2002, **47**, 3595–3609.
- 5 M. Englisch, A. Jentys and J. A. Lercher, *J. Catal.*, 1997, **166**, 25–35.
- 6 I. Lee, R. Morales, M. A. Albiter and F. Zaera, *Proc. Natl. Acad. Sci. U. S. A.*, 2008, **105**, 15241–15246.
- 7 D. Loffreda, F. Delbecq, F. Vigne and P. Sautet, *J. Am. Chem. Soc.*, 2006, **128**, 1316–1323.
- 8 C. K. Tsung, J. N. Kuhn, W. Y. Huang, C. Aliaga, L. I. Hung, G. A. Somorjai and P. D. Yang, *J. Am. Chem. Soc.*, 2009, **131**, 5816–5822.
- 9 K. M. Bratlie, H. Lee, K. Komvopoulos, P. D. Yang and G. A. Somorjai, *Nano Lett.*, 2007, **7**, 3097–3101.
- 10 E. Herrero, K. Franaszczuk and A. Wieckowski, *J. Phys. Chem.*, 1994, **98**, 5074–5083.
- 11 A. C. Chen and P. Holt-Hindle, *Chem. Rev.*, 2010, **110**, 3767–3804.
- 12 C. R. K. Rao and D. C. Trivedi, *Coord. Chem. Rev.*, 2005, **249**, 613–631.
- 13 J. Y. Chen, B. Lim, E. P. Lee and Y. N. Xia, *Nano Today*, 2009, **4**, 81–95.
- 14 Z. M. Peng and H. Yang, *Nano Today*, 2009, **4**, 143–164.
- 15 J. T. Ren and R. D. Tilley, *J. Am. Chem. Soc.*, 2007, **129**, 3287–3291.
- 16 A. R. Tao, S. Habas and P. D. Yang, *Small*, 2008, **4**, 310–325.
- 17 N. Tian, Z. Y. Zhou, S. G. Sun, Y. Ding and Z. L. Wang, *Science*, 2007, **316**, 732–735.
- 18 T. S. Ahmadi, Z. L. Wang, T. C. Green, A. Henglein and M. A. ElSayed, *Science*, 1996, **272**, 1924–1926.
- 19 H. Lee, S. E. Habas, S. Kwekin, D. Butcher, G. A. Somorjai and P. D. Yang, *Angew. Chem., Int. Ed.*, 2006, **45**, 7824–7828.
- 20 H. Song, F. Kim, S. Connor, G. A. Somorjai and P. D. Yang, *J. Phys. Chem. B*, 2005, **109**, 188–193.
- 21 C. Wang, H. Daimon, Y. Lee, J. Kim and S. Sun, *J. Am. Chem. Soc.*, 2007, **129**, 6974–6975.
- 22 J. Zhang and J. Y. Fang, *J. Am. Chem. Soc.*, 2009, **131**, 18543–18547.
- 23 Y. J. Kang, X. C. Ye and C. B. Murray, *Angew. Chem., Int. Ed.*, 2010, **49**, 6156–6159.
- 24 B. H. Wu, N. F. Zheng and G. Fu, *Chem. Commun.*, 2011, **47**, 1039–1041.
- 25 J. B. Wu, A. Gross and H. Yang, *Nano Lett.*, 2011, **11**, 798–802.
- 26 L. Palaikis, D. Zurawski, M. Hourani and A. Wieckowski, *Surf. Sci.*, 1988, **199**, 183–198.
- 27 F. C. Collins and G. E. Kimball, *J. Colloid Sci.*, 1949, **4**, 425–437.
- 28 D. C. Torney and H. M. McConnell, *Proc. R. Soc. London, Ser. A*, 1983, **387**, 147–170.
- 29 H. Van Beijeren, W. Dong and L. Bocquet, *J. Chem. Phys.*, 2001, **114**, 6265–6275.